
The Raman spectra of left-handed DNA oligomers incorporating adenine-thymine base pairs⁺

J.M.Benevides¹, A.H.-J.Wang², G.A.van der Marel³, J.H.van Boom³, A.Rich² and G.J.Thomas, Jr.^{1,*}

¹Department of Chemistry, Southeastern Massachusetts University, North Dartmouth, MA 02747,

²Department of Biology, Massachusetts Institute of Technology, Cambridge, MA 02139, USA, and

³Gorlaeus Laboratories, University of Leiden, 2300 RA Leiden, The Netherlands

Received 13 April 1984; Revised and Accepted 18 June 1984

ABSTRACT

Raman spectra were obtained from single crystals of $[d(\text{CGCATGCG})]_2$ and $[d(m^5\text{CGTAm}^5\text{CG})]_2$, both of which incorporate A-T pairs into Z-DNA structures and contain C2'-endo/syn conformers of deoxyguanosine at the oligonucleotide ends. Correlation with x-ray results permits the following Raman assignments for nucleoside conformers: C3'-endo/syn G, 623±1; C2'-endo/syn G, 671±2; C2'-endo/anti C, 782±1; C2'-endo/anti T, 650±5 and ca. 750; C3'-endo/syn A, 729±1 cm^{-1} . These results show that (i) the 670 cm^{-1} line of syn G is highly sensitive to the change from C3'-endo to C2'-endo pucker, (ii) the 729 cm^{-1} line of A is affected neither by furanose pucker nor glycosidic bond orientation and (iii) the 1200-1500 cm^{-1} region of the Raman spectrum of the A-T double helix is greatly altered by the B-to-Z transition. Conformation sensitive Raman frequencies in the 850-1700 cm^{-1} region are identified for both octamer and hexamer, and the Z-to-B transition of each is monitored by spectral changes which occur upon dissolving the crystal in H₂O solution.

INTRODUCTION

Single crystal x-ray analysis is a powerful tool for the elucidation of DNA oligonucleotide structures (1). The results obtained on crystalline samples also suggest possible conformations for nucleotides in aqueous nucleic acids (2). Nevertheless, other experimental methods are required to investigate directly the nucleotide conformations in aqueous DNA and RNA. Laser Raman spectroscopy, like nuclear magnetic resonance (NMR) and circular dichroism (CD) methods, has been particularly useful in conformational analysis of nucleic acids under sampling conditions which closely approximate those *in vivo* (3). The Raman spectroscopic method requires for implementation, however, a library of spectra corresponding to models of well characterized structure. It is therefore desirable to obtain the Raman spectra of nucleic acid models of precisely defined structure and sequence, such as those recently subjected to high resolution, single crystal x-ray diffraction analysis.

In this paper we report the laser Raman spectra of two self-complementary DNA crystals, $[d(\text{CGCATGCG})]_2$ and $[d(m^5\text{CGTAm}^5\text{CG})]_2$. The Raman data obtained from the crystals are compared both with the x-ray results obtained from the

same crystals and with Raman data obtained from aqueous solutions of these and related DNA models. Knowledge of the detailed molecular structures within the crystals permits the observed Raman bands to be assigned unambiguously to specific nucleotide conformers of A, G, C, and T. The "conformation-marker" bands which are thus identified can be utilized for conformation characterization in DNA samples of unknown structure. Since the Raman data are transferable between crystalline and non-crystalline states, the present results are not limited to applications involving crystalline samples but are generally applicable to aqueous DNA.

We also report here for the first time the Raman spectra of A-T base pairs which have been incorporated into a left-handed Z-DNA helix. By use of computer subtraction techniques, we have generated a hypothetical Raman spectrum corresponding to a Z-DNA structure containing only A and T bases in extended and alternating sequence. The present results suggest that the Raman spectrum can be profitably exploited to distinguish Z and B conformers of AT-containing DNAs in a fashion similar to that demonstrated previously for GC-containing DNAs (4,5).

MATERIALS AND METHODS

Synthesis of Self-Complementary Oligonucleotides.

Both of the DNA oligonucleotides, d(m⁵CGTAm⁵CG) and d(CGCATGCG), were synthesized by an improved phosphodiester technique in which 1-hydroxybenzotriazol was used as an activating reagent (6). After the deblocking of the fully protected molecules, both fragments were purified by Sephadex G50 column chromatography and converted into ammonium salts. The purity of each oligomer was greater than 95%, as judged by HPLC analysis. The crystallization and structural analyses of these molecules have been described in detail elsewhere (7,8) and are reviewed briefly here.

Growth of Single Crystals and X-Ray Diffraction.

The DNA fragments were crystallized using the vapor diffusion technique with 2-methyl-2,4-pentanediol as the precipitating agent. The methylated hexamer crystallized in the orthorhombic space group P2₁2₁2₁, isomorphous to the original Z-DNA lattice of [d(CGCGCG)]₂ (9). The structure has been refined to an R-factor of 0.17 at a resolution of 1.2Å. The structure of the molecule is similar to that of the left-handed Z-DNA double helix [d(CGCGCG)]₂ (9).

The octamer, d(CGCATGCG), crystallized in the hexagonal space group P6₅ which is isomorphous to that of the tetramer, d(CGCG) (10). The crystalliza-

tion was facilitated by raising the initial $MgCl_2$ concentration in the crystallization medium to 500mM. The structure has been refined to an R-factor of 0.21 at 2.5Å resolution. Due to statistical disorder of the hexagonal lattice, the resolution of the structure determination in this crystal is somewhat inferior to that of the orthorhombic lattice. Nevertheless, it is quite clear that the octamer exists completely in the Z-DNA conformation.

Raman Spectroscopy.

The octamer or hexamer crystal, authenticated by x-ray diffraction as referenced in the preceding section, was transferred with approximately 10 μ l of mother liquor (2-methyl-2,4-pentanediol (40%) + 25mM sodium cacodylate (pH7) + 2mM spermine + 10mM $MgCl_2$) to a Raman sample cell (Kimax #34507 glass capillary) which was thermostated at 32°C. The 514.5nm line from a Coherent Model CR-2 argon laser was focussed on the crystal and the Raman scattering at 90° was collected and analyzed by a Spex Ramalog spectrometer under the control of a North Star Horizon II microcomputer. Spectral data were collected at 1.0 cm^{-1} intervals with an integration time of 1.5 sec. A slit width of 8.0 cm^{-1} was employed for each scan of the spectrum from 300 to 1800 cm^{-1} . Spectra of solutions of the oligomers (7mM) were obtained similarly.

Each Raman spectrum displayed below is the average of several scans, of 1.5 cm^{-1} or less repeatability, from which the fluorescent background and scattering by the solvent or mother liquor have been removed using computer subtraction techniques (11,12). The spectrum of solvent or mother liquor was always recorded with the same instrument settings employed for solution or crystal. The procedure is illustrated in Fig. 1. It will be noted from the topmost spectrum of Fig. 1 that the most intense Raman line of the mother liquor occurs at 763 cm^{-1} , sufficiently well removed from the DNA lines at 750 and 782 cm^{-1} to permit precise subtraction of mother liquor contributions to the crystal spectrum, well within the limits of the overall signal-to-noise ratio of the data (approximately 10:1). The second from top spectrum of Fig. 1 shows in fact that the mother liquor contributes very little to the Raman spectrum of the suspended crystal irrespective of computer subtraction, which is a consequence of the relatively dense packing of the solid in the Raman sample cell. Proper compensation by spectral subtraction is confirmed also by the absence from the Fig. 1 spectrum of Z-DNA (bottom) of other relatively prominent Raman lines of the mother liquor, such as that at 835 cm^{-1} .

In some of the spectra the noise was smoothed by a least squares fit of third order polynomials to overlapping fifteen point regions (13). This

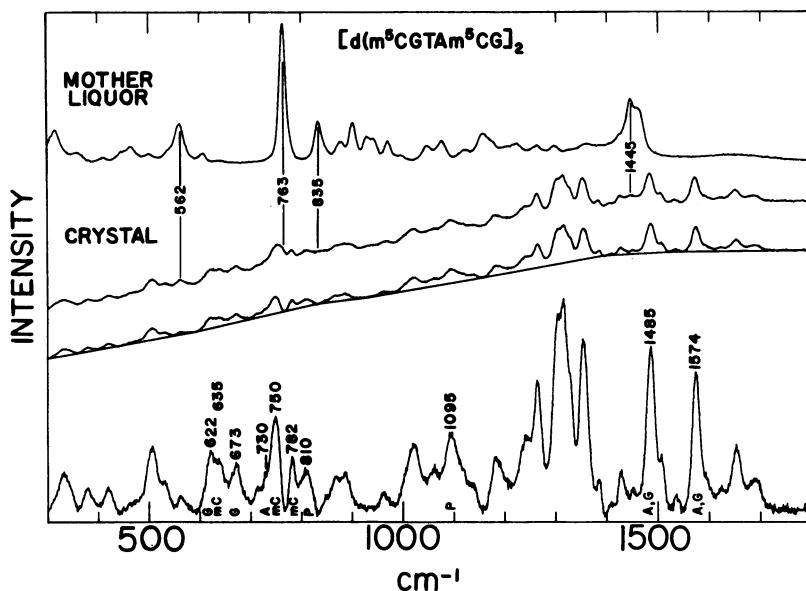


Figure 1: From top to bottom: Raman spectra of mother liquor (2-methyl-2,4-pentanediol (40%) + 25mM sodium cacodylate (pH7) + 2mM spermine + 10mM $MgCl_2$); crystalline hexamer $[d(m^5CGTAm^5CG)]_2$; crystalline hexamer corrected for mother liquor; and crystalline hexamer corrected for both mother liquor and fluorescent background. Prominent lines of the bases and backbone are labelled by the symbols A, C, G, T and P, respectively, in the bottom spectrum. Vertical lines denote positions of Raman peaks due to mother liquor which appear weakly in the spectrum of the crystal (second from top).

procedure did not measurably alter the Raman line frequencies or intensities.

Computation of Raman difference spectra between different DNA structures was carried out as described previously (5,11). Our method involves use of the strong purine line near 1575 cm^{-1} as the intensity normalization standard. The advantages of this method have been discussed in detail (11).

RESULTS

Background and Solvent Corrections to Raman Spectra

The top spectrum of Fig. 1 is that of the mother liquor. In the next trace (second from top), the Raman spectrum of the hexamer crystal is displayed as recorded by averaging six successive scans of the $300\text{ to }1800\text{ cm}^{-1}$ region. The raw data contain the Raman scattering from both $[d(m^5CGTAm^5CG)]_2$ and mother liquor (vertical lines), as well as an ascending background which most probably results from a trace fluorescent impurity in the hexamer. In

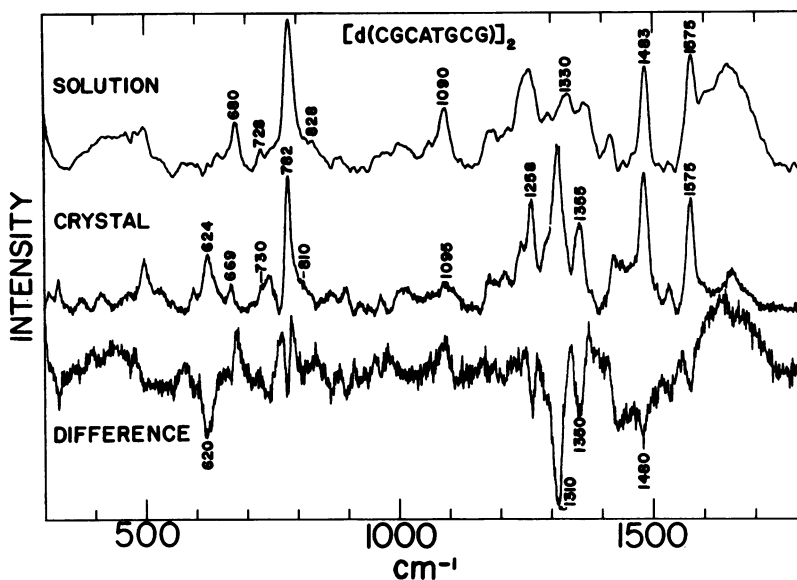


Figure 2: Raman spectra of the octamer $[d(CGCGATGCG)]_2$ in aqueous solution (top, 15-point smoothed), in the crystalline state (middle), and the difference between solution and crystal (bottom). Lines are labeled as in Fig. 1.

the next spectrum (second from bottom) the bands of the mother liquor have been removed by computer subtraction, as described above (Materials and Methods Section). The baseline drawn in this spectrum connects well defined minima for subsequent subtraction of the background fluorescence. In the bottom trace of Fig. 1, the fully corrected Raman spectrum of the hexamer is shown on an amplified scale. Note that no smoothing of noise has been employed to refine the bottom trace of Fig. 1. Similar data reductions were carried out for the octamer crystal and for solutions of hexamer and octamer, except that smoothing of excessive spectral noise was sometimes required as indicated in the appropriate Figure legends.

$[d(CGCGATGCG)]_2$

Fig. 2 shows the Raman spectra of $[d(CGCGATGCG)]_2$ in the region 300-1800 cm^{-1} for the solution (top), the crystal (middle) and their difference (bottom). The difference spectrum has been plotted in the "solution-minus-crystal" format for consistency with the "B-minus-Z" difference spectrum of poly(dG-dC) published previously (5).

$[d(m^5CGTAm^5CG)]_2$

Fig. 3 shows the Raman spectra of $[d(m^5CGTAm^5CG)]_2$ in the solution (top)

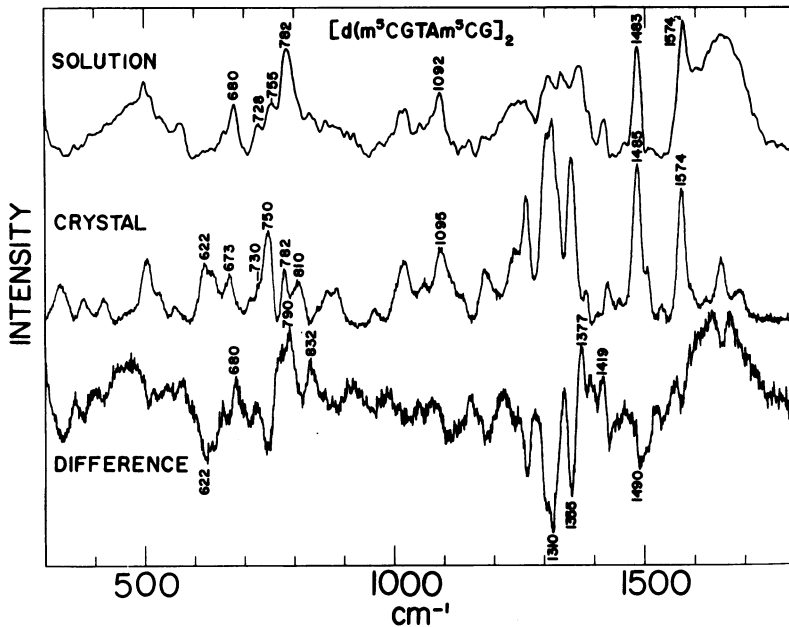


Figure 3: Raman spectra of the hexamer $[d(m^5CGTAm^5CG)_2]$ in aqueous solution (top, 15-point smoothed), in the crystalline state (middle) and the difference between solution and crystal (bottom). Lines are labelled as in Fig. 1.

and crystal (middle) states, and the solution-minus-crystal difference spectrum (bottom). Because the Raman spectrum is highly sensitive to primary molecular structure, the inclusion of the chemically modified pyrimidine, 5-methylcytosine (m^5C), in the hexamer sequence is expected to have a profound effect on the spectrum, irrespective of secondary structure effects. Accordingly, we include for comparison in Fig. 4 the Raman spectra of deoxycytidine-5'-monophosphate and 5-methyldeoxycytidine-5'-monophosphate. Inspection of Fig. 4 reveals the characteristic Raman lines of the m^5C residue which distinguish it from the normal cytosine ring in monomers at the same experimental conditions. The prominent Raman lines of the m^5C residues in the hexamer spectra (Fig. 3) are thus readily assigned by reference to Fig. 4.

DISCUSSION

Assignment of Raman Frequencies in the Region 600-850 cm^{-1} .

X-ray data show that octamer (8) and hexamer crystals (7) both contain

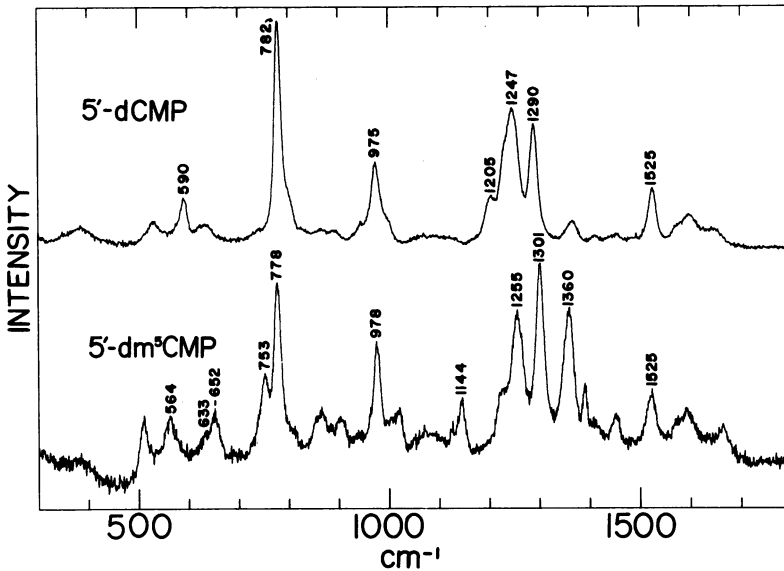
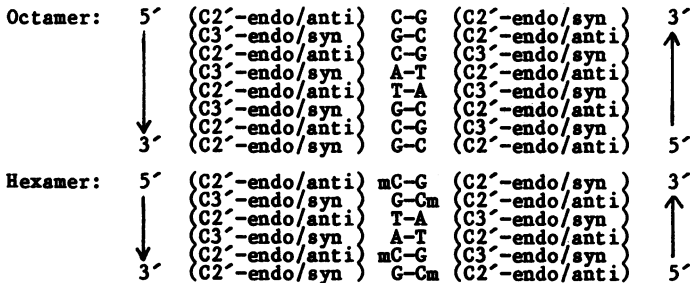


Figure 4: Raman spectra of 0.10M solutions of deoxycytidine-5'-mophosphate (5'-dCMP) and 5-methyldeoxycytidine-5'-monophosphate (5'-dm³CMP) each at pH7. Spectra are corrected for scattering by solvent.

left-handed Z-DNA. Nucleotide conformations corresponding to these sequences are as follows:



On the basis of the x-ray results summarized above and extensive Raman studies of model compounds (14,15), we expect for each crystal two Raman lines in the 620-680 cm⁻¹ interval corresponding to the two conformers of G, and one line in the vicinity of 730 cm⁻¹ corresponding to the C3'-endo/syn conformer of A. The Raman lines appearing in the octamer crystal at 624 and 669 cm⁻¹ and in the hexamer crystal at 622 and 673 cm⁻¹ are therefore assigned confidently to the two G conformers of Z-DNA as summarized in Table 1. The Raman line which occurs near 730 cm⁻¹ in each crystal is also assigned

TABLE 1^aRAMAN FREQUENCIES AND ASSIGNMENTS FOR NUCLEOTIDE CONFORMERS
OF [d(CGCATGCG)]₂ AND [d(m⁵CGTAm⁵CG)]₂

| <u>Base (Conformer)</u> | <u>Octamer</u> | | <u>Hexamer</u> | |
|-------------------------|---------------------------------|----------------------------------|---------------------------------|--|
| | <u>Crystal</u> <u>Z-Form</u> | <u>Solution</u> <u>B-Form</u> | <u>Crystal</u> <u>Z-Form</u> | <u>Solution</u> <u>B-Form</u> |
| G (C3'-endo/syn) | 624 | | 622 | |
| G (C2'-endo/syn) | 669 | | 673 | |
| G (C2'-endo/anti) | | 680 | | 680 |
| A (C3'-endo/syn) | (730) | | 730 | |
| A (C2'-endo/anti) | | 728 | | 728 |
| C (C2'-endo/anti) | 781 | 782 | | |
| mC (C2'-endo/anti) | | | (635) (750)* 782 | (655) (755) 783 |
| T (C2'-endo/anti) | (660) ⁺ (750)* | 645 (750) | (662) ⁺ (750)* | (650) ⁺ (755) ⁺ |

^aFrequencies are accurate to ± 2 cm^{-1} , except values in parentheses which are estimated to ± 5 cm^{-1} . Asterisks denote Raman lines which are partially overlapped by the strong 763 cm^{-1} line of mother liquor. (See Fig. 1.) Daggers indicate lines which are partially overlapped by other lines of the oligomer.

unambiguously to the internal C3'-endo/syn A conformer.

The Z-DNA assignments are confirmed by the band shifts which result upon dissolving the crystals in aqueous solution, whereupon the oligomers assume the conventional B-DNA secondary structure. Thus, as shown in the difference spectra of Figs. 2 and 3, the pair of lines assigned to the syn guanines coalesce into a single line at 680 cm^{-1} , which is characteristic of the C2'-endo/anti G conformer of B-DNA (11,16). On the other hand, the 730 cm^{-1} line of A is barely shifted (to 728 cm^{-1}) by the Z-to-B transition. Assignments of the remaining purine and pyrimidine ring modes of Z and B forms of the octamer and hexamer are included in Table 1. The tabulation shows that the prominent ring mode of C (and m⁵C) near 782 cm^{-1} is unaffected by the Z-to-B transition, whereas the weaker band of T near 650 cm^{-1} is not sufficiently well resolved from the overlapping guanine line to determine whether or not the frequency is sensitive to the secondary structure transition. X-ray results show that neither C nor T nucleotides undergo substantial changes in furanose pucker or glycosidic bond orientation with the Z-to-B transition. Therefore, on the basis of the x-ray findings, significant changes in the pyrimidine Raman lines

are not expected to occur.

The Raman frequencies associated with vibrations of the deoxyribose-phosphate backbone of Z and B oligomer structures (Figs. 2 and 3) are consistent with those reported previously for poly(dG-dC) (4,5,17). However, as expected, the lines are somewhat less intense in the oligomers than in the polymer.

Intensities of the Raman Lines of Syn Conformers of Guanine.

Figs. 2 and 3 show that the ratio of peak heights of the lines assigned to C3'-endo/syn and C2'-endo/syn conformers of G, i.e. the quotient I_{623}/I_{671} , has the value 2.6:1 in the octamer and 1.4:1 in the hexamer. (Similar quotients are computed from ratios of the corresponding integrated band areas.) Theoretically, we expect the I_{623}/I_{671} ratio in octamer and hexamer crystals to exhibit the values 2:1 and 1:1, respectively, corresponding to the actual number ratio of internal to terminal G residues in each oligomer. We assume, of course, that the Raman lines of the two conformers have the same intrinsic intensities, an approximation which is demonstrably valid for 5'-rGMP and 5'-dGMP mononucleotides (15). The fact that the observed and expected values of I_{623}/I_{671} are relatively close to one another supports the band assignments given in the preceding section. The fairly intense line of m^5C near 635 cm^{-1} in the hexamer and "hidden" lines in the $600\text{--}630\text{ cm}^{-1}$ region of the octamer may well account for the somewhat greater than expected intensity ratios.

The B-to-Z Secondary Structure Transitions and Raman Lines of the Region 850-1750 cm^{-1} .

Raman difference spectroscopy was employed previously to demonstrate all of the spectral changes which accompany the B-to-Z transition in poly(dG-dC) (5). The bands in the $850\text{--}1750\text{ cm}^{-1}$ region were shown to be among the most sensitive in position and intensity to the change in DNA secondary structure. However, because these bands substantially overlap one another, they are somewhat less useful for quantitative analysis of DNA structure transitions. Here we draw attention to the qualitative features or "profile" of the $850\text{--}1750\text{ cm}^{-1}$ region in difference spectra of Figs. 2 and 3, particularly the deep troughs near 1310 and 1350 cm^{-1} , and the shallower trough near 1500 cm^{-1} .

The profile observed for each oligomer closely matches that reported for poly(dG-dC), with one exception: In the polymer, the B-minus-Z difference spectrum contains an intense peak near 1492 cm^{-1} which clearly is absent from difference spectra of Figs. 2 and 3. This can be attributed to the negligible shift in frequency of the G line near 1490 cm^{-1} for the oligomer transitions,

as opposed to the substantial shift of the line to lower frequency for the polymer transition. The present results indicate either a much smaller perturbation of the G ring mode from stacking of the bases in the B-DNA oligomers than that observed in the B-DNA polymer, or conversely, a greater perturbation in the oligomeric Z-DNA structures. If either interpretation is correct, it would suggest a sequence and/or helix-length dependence of the guanine ring frequency near 1490 cm^{-1} which could be exploited for secondary structure analysis.

Finally, we emphasize that the secondary structure transitions of the oligomers result in the identical spectral changes observed for poly(dG-dC) in the $600\text{--}850\text{ cm}^{-1}$ region (cf. Figs. 2 and 3, above, with Fig. 3 of ref.(5)). The Raman Spectrum of a Hypothetical Z-DNA Containing Only A-T Base Pairs in Alternating Sequence.

Although various studies have postulated the stability of a left-handed DNA double helix containing exclusively A-T pairs in alternating sequence (18), the Z-DNA structure has been demonstrated experimentally only for systems containing no more than 50% A-T pairs, such as poly(dA-dm⁵C)·poly(dG-dT) (19). Therefore, the Raman spectrum of a Z-DNA containing only A-T pairs is not known. Interest in such a spectrum arises not only for its obvious use in secondary structure analysis, but also for gaining a better understanding of the different vibrational interactions which occur in the B and Z structures.

In Fig. 5 we show the Raman difference spectrum which results from subtracting the spectrum of the well known Z-DNA hexamer [d(CGCGCG)]₂ from that of the present Z-DNA octamer [d(CGCATGCG)]₂. The CG hexamer spectrum is identical to that published previously (4), and the contributions of its CG pairs, including end effects (see below), are indistinguishable from those in the spectrum of the octamer. Accordingly, the difference spectrum of Fig. 5 should correspond to that of the two internal and sequence-alternating A-T pairs of the octamer, i.e. a Z-DNA containing exclusively A-T pairs. (Note also that Raman lines due exclusively to backbone vibrations, such as the 1095 cm^{-1} line of PO_2^- , are totally removed by subtraction and therefore will not appear in the difference spectrum.)

The Raman spectrum of the B-form of poly(dA-dT)·poly(dA-dT) is included in Fig. 5 for comparison with the hypothetical Z structure. The present results indicate a striking change in the AT spectrum attendant with the B-to-Z structure transition. Specifically, the intense adenine and thymine lines

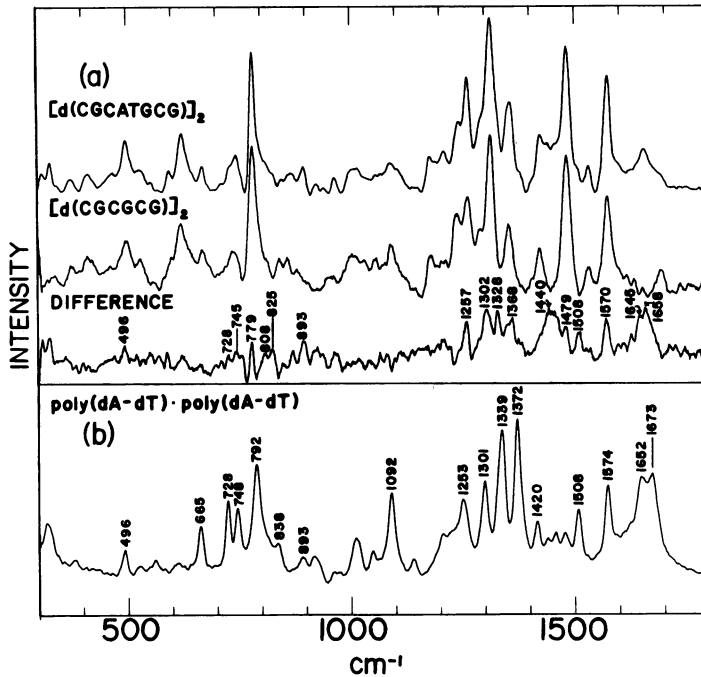


Figure 5: (a) Raman spectra of the crystalline octamer $[d(CGCGATGCG)]_2$ (top), the crystalline hexamer $[d(CGCGCG)]_2$ (middle) and their difference spectrum (bottom). (b) Raman spectrum of the B-form of aqueous $\text{poly}(dA-dT) \cdot \text{poly}(dA-dT)$. All spectra in (a) have been smoothed.

of the $1200\text{--}1500\text{ cm}^{-1}$ interval yield different profiles in the two structures. A further refinement of the AT data and more detailed comparison with the corresponding GC data will be given elsewhere.

CONCLUSIONS

Characterization of Nucleotide Conformation from Raman Spectra.

The combined x-ray and Raman results indicate that the guanine conformers, $C3'$ -endo/syn (Z-helix, internal residue) and $C2'$ -endo/syn (Z-helix, terminal residue), are distinguished from one another and from $C2'$ -endo/anti guanine (B-helix) by their respective Raman lines at 623, 671 and 680 cm^{-1} . We note, as well, that the ring mode of $C3'$ -endo/anti guanine (A-helix) occurs near 668 cm^{-1} (15), and therefore this conformer could not be easily distinguished from $C2'$ -endo/syn guanine by reliance only on the Raman line near 670 cm^{-1} .

Unlike guanine, adenine exhibits no Raman line in the 600–850 cm^{-1} region which is sensitive to nucleotide conformation. In addition, the Raman lines of the pyrimidines in this region are not altered by pairing to *syn* purines. An explanation for the unique sensitivity of the guanine ring mode to nucleotide conformation has been given previously (15). On the other hand, the intense lines of adenine, cytosine and thymine in the 1200–1500 cm^{-1} region, like those of guanine, are not invariant to secondary structure differences and yield characteristic profiles for B and Z helices.

The phosphodiester backbone of the Z form of poly(dG–dC) exhibits characteristic Raman lines at 748, 792, 810, 1095 and 1425 cm^{-1} (5). The last three of these are observed in Z structures of the hexamer and octamer crystals, and the first two may be presumed present though obscured by coincident ring frequencies of the pyrimidines. The present data are therefore consistent with and confirmatory of the Raman assignments proposed earlier (5).

Comment on the Assignment of the 671 cm^{-1} Line to C2'-endo/*syn* Guanine.

In the previous Raman study of the single crystal of [d(CGCGCG)]₂, (4), the guanine line ca. 675 cm^{-1} could not be assigned a priori to a specific conformer although its intensity relative to that of the companion guanine line ca. 625 cm^{-1} (0.4:1.0) suggested its origin in the terminal residues. Thamann & al. proposed, therefore, that the 625 and 675 cm^{-1} lines should be assigned to internal and terminal guanines, respectively. The present results (actual frequencies: 623 and 671 cm^{-1}) confirm the earlier assignments and show further that the terminal guanines of [d(CGCGCG)]₂ assume the C2'-endo/*syn* conformation in common with terminal guanines of both [d(GGCATGCG)]₂ and [d(m⁵CGTAm⁵CG)]₂.

ACKNOWLEDGEMENTS: This work was supported by National Institutes of Health Grant A118758 (to G.J.T.), by grants from the National Institutes of Health, American Cancer Society and National Aeronautics and Space Administration (to A. R.), and by The Netherlands Organization for the Advancement of Pure Research (ZWO) (to J. H. vB.).

*To whom correspondence may be addressed

+ This is part XXVI in the series Raman Spectral Studies of Nucleic Acids. Paper XXV in this series is Benevides, J.M. and Thomas, G.J., Jr. (1983) *Nucleic Acids Res.*, **11**, 5747-5761.

REFERENCES

1. Wang, A. H.-J., Fujii, S., van Boom, J. H. and Rich, A. (1983) Cold Spring Harbor Symp. Quant. Biol. 47, 33-44.
2. Dickerson, R. E., Drew, H. R., Conner, B. N., Kopka, M. L. and Pjura, P. J. (1982) Cold Spring Harbor Symp. Quant. Biol. 47, 13-24.
3. Thomas, G. J., Jr. and Kyogoku, Y. (1977) Pract. Spectrosc. 1C, 717-872.
4. Thamann, T., Lord, R. C., Wang, A. H. J., and Rich, A. (1981) Nucl. Acids Res. 9, 5443-5457.
5. Benevides, J. M. and Thomas, G. J., Jr. (1983) Nucl. Acids Res. 11, 5747-5761.
6. van der Marel, G. A., van Boeckel, C. A. A., Wille, G. and van Boom, J. H. (1981) Tetrahedron Lett. 3887.
7. Wang, A. H.-J., Hakoshima, T., van der Marel, G. A., van Boom, J. H. and Rich, A. (1984) (submitted).
8. Fujii, S., Wang, A. H.-J., Quigley, G. J., Westerink, H., van der Marel, G. A., van Boom, J. H. and Rich, A. (1984) (submitted).
9. Wang, A. H.-J., Quigley, G. J., Kolpak, F. J., Crawford, J. L., van Boom, J. H., van der Marel, G. and Rich, A. (1979) Nature 282, 680-686.
10. Crawford, J. L., Kolpak, F. J., Wang, A. H.-J., Quigley, G. J., van Boom, J. H., van der Marel, G. and Rich, A. (1981) Proc. Natl. Acad. Sci. USA 77, 4016-4020.
11. Prescott, B., Steinmetz, W. and Thomas, G. J., Jr. (1984) Biopolymers 23, 235-256.
12. Li, Y., Thomas, G. J., Jr., Fuller, M. and King, J. (1981) Prog. Clin. Biol. Res. 64, 271-283.
13. Savitzky, A. and Golay, M. J. E. (1964) Anal. Chem. 36, 1627-1639.
14. Lord, R. C. and Thomas, G. J., Jr. (1967) Spectrochim. Acta 23A, 2551-2591.
15. Benevides, J. M., LeMeur, D. and Thomas, G. J., Jr. (1984) Biopolymers 23, 1011-1024.
16. Nishimura, Y., Tsuboi, M., Nakano, T., Higuchi, S., Sato, T., Shida, T., Uesugi, S., Ohtsuka, E. and Ikehara, M. (1983) Nucl. Acids Res. 11, 1579-1588.
17. Pohl, F. M., Ranade, A. and Stockburger, M. (1973) Biochim. Biophys. Acta 335, 85-92.
18. Sarma, R. H., Ed. (1981) Biomolecular Stereodynamics, Volume 1, Adenine Press, New York.
19. McIntosh, L. F., Grieger, I., Eckstein, F., Zarling, D. A., van de Sande, J. H. and Jovin, T. M. (1983) Nature 304, 83-86.